

WAVEGUIDE PROPERTIES OF A FILM WITH A PARABOLIC PROFILE OF THE REFRACTIVE INDEX EMBEDDED IN A MEDIUM WITH PHOTOREFRACTIVE NONLINEARITY

S.E. SAVOTCHENKO^{1,2}

¹ MIREA - Russian Technological University,
Vernadsky Ave, 78, 119454, Moscow, Russia

² Moscow Technical University of Communications and Informatics,
Aviamotornaya st., 8A, 111024, Moscow, Russia

Received September 4, 2025

Abstract. Waveguide properties of a film with a parabolic spatial profile of the refractive index inserted in a medium with diffusion type of photorefractive nonlinearity are described theoretically. Two new types of guided waves with a spatial profile localized along the film boundaries are found. Exact solutions to the wave equation corresponding to even and odd modes are obtained. The wave of the first type attenuates with oscillations in the photorefractive coating media, whereas the wave of the second type attenuates without oscillations. The two wave types also differ from each other by the range of values of the propagation constant. The obtained modes exist at certain discrete values of the propagation constant, which depend on the optical parameters of the system and the film thickness. The total power flow of all types of modes is calculated and the effect of the film thickness is analyzed. Waveguide modes can only be excited when the energy of the exciting beam is greater than the critical value of the wave total power flow. A large fraction of the energy is concentrated in the photorefractive plates at small film thicknesses. The redistribution of energy between the film and the photorefractive plates occurs with an increase in the film thickness.

Key words: wave equation; Helmholtz equation; mathematical modeling; nonlinear optics; photorefractive crystal; boundary value problem; nonlinear waves; guided waves; waveguide optics; transverse wave.

1. INTRODUCTION

Planar optical waveguides are studied intensively for a long time [1]. The widespread use of such waveguides [2] is due to the fact that they are made of both crystalline [3] and polymeric materials [4].

Optical waveguides are usually step-index, graded-index, and nonlinear ones. The step-index waveguides are characterized by the constant value of the refractive index at any distances across the guided layer direction. The refractive index depends on the spatial distance in the graded-index waveguides [5]. The nonlinear waveguides are characterized by the dependence of the refractive index on the light intensity [6].

Various forms of nonlinear responses are studied. Most often used nonlinearity is the Kerr type one [7]. In particular, the authors of [8] report TM wave analysis of vertically coupled optical micro ring resonator with Kerr type nonlinear cladding. The author of [9] reports a theory of guided TE modes in a one-dimensional slab waveguide bounded by nonlinear media with intensity dependent refractive indices.

Nonlinear waves in waveguide structures formed of a saturable intensity dependent refractive index are also studied well [10]. Electromagnetic wave propagation in the waveguides with power nonlinearity is described theoretically in [11]. Step-wise nonlinear response is used in [12]. Generalizations of the stepwise intensity-dependent nonlinearity are proposed in [13, 14], including the three-layered waveguide structures [15]. Waveguide properties of the photorefractive slab crystals are studied in [16] including diffusion mechanism of such nonlinearity formation [17].

Gradient (graded-index) waveguides differ from each other by the refractive index profile [18]. An arbitrary refractive index profile in planar waveguides requires the use of special numerically accurate [19] and precise analytical methods [20]. Exact analytical solution describing modes in the graded-index waveguides are obtained in the case of linear [21], exponential [22], parabolic [23], saturable [24] spatial profiles of the refractive index (or dielectric constant).

Of greatest practical interest are layered waveguide structures both nonlinear [25, 26] and graded-index [27] ones. However, the properties of waveguides combining graded-index and nonlinear layers have not been studied enough [28]. In particular, exact analytical solutions of TE and TM modes of a slab waveguide with a nonlinear covering medium and an exponential graded-index thin film are obtained in [29, 30]. Recently, we actively began to study the waveguide properties of the interfaces between graded-index and nonlinear media with different forms of nonlinear responses [31] including the photorefractive one [32].

In this paper, we consider the symmetrical waveguide structure similar to that described in [33] in the case of the linearly graded-index film in the photorefractive crystal. Here we use a parabolic [34] (instead of linear [33]) profile of the refractive index of the film inserted in the photorefractive crystal. We focus on the effect of the film thickness of the wave energy flow distribution across the film boundaries direction [35]. Many authors noted the importance of the influence of the thickness of an interlayer or coating on the waveguiding properties of layered structures [36] including multilayer graded-index planar waveguide [37, 38].

This paper is organized as follows. The main equations of the model of a symmetric film waveguide and the boundary value problem formulation are

presented in Sec. 2. Exact solutions to the boundary value problem describing the waves with oscillations in photorefractive medium are given in Sec. 3. Exact solutions to the boundary value problem describing the waves without oscillations in photorefractive medium are presented in Sec. 4. The results of the power flow calculations are given in Sec. 5. Discussion and the comparison of the obtained results are presented in Sec. 6. The conclusions are contained in Sec. 7.

2. EQUATIONS OF A SYMMETRIC FILM WAVEGUIDE

We consider the nonmagnetic lossless symmetrical waveguide structure schematically plotted in Fig. 1. The planar film (waveguide core) with a parabolic profile of the refractive index of $2a$ thickness is separated by semi-infinite crystals (coating media) with the diffusion type of photorefractive nonlinearity and oppositely oriented polar axes.

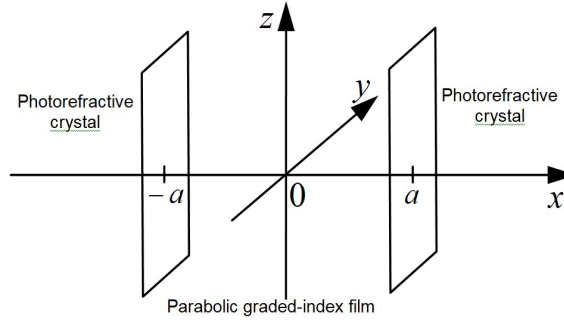


Fig. 1. Scheme of symmetric waveguide system.

Let us choose x -axes in the direction perpendicular to the film boundaries, which are planar and located at the planes $x = \pm a$. We will consider the monochromatic waves propagating along z -axes supposing that the electromagnetic field is homogeneous along the film waveguide.

Let us write the refractive index of symmetric film waveguide as

$$n(x, I) = \begin{cases} n_p(I), & |x| > a, \\ n_G(x), & |x| < a, \end{cases} \quad (1)$$

where the refractive index of the film with a parabolic profile can be presented as

$$n_G^2(x) = n_{G0}^2 \{1 - \Delta(x/a)^2\}$$

Here n_{G0} is the initial value of the refractive index at film center (at $x=0$), $\Delta = (n_{G0}^2 - n_{Ga}^2)/n_{G0}^2$, where n_{Ga} is the refractive index at the film boundaries (at $x = \pm a$) [33, 34, 39].

The refractive index of the medium with photorefractive nonlinearity can be presented as

$$n_p(I) = n_{p0} + \Delta n(I),$$

where I is the light intensity, n_{p0} is the unperturbed refractive index, and $\Delta n(I)$ is a small additive term ($\Delta n(I) \ll n_{p0}$). The additive term Δn in the case of diffusion mechanism of photorefractive nonlinearity formation can be written as [17, 40]

$$\Delta n(I) = \text{sign}(x) n_{p0}^3 r_{eff} (k_B T / 2e) I' / (I + I_d),$$

where r_{eff} is the effective electro-optic coefficient, k_B is Boltzmann constant, T is a temperature, e is the modulus of the electron charge, I' is the derivative of the light intensity, I_d is the dark intensity, which is assumed to be a small one ($I_d \ll I$).

The lightwave propagation is described by the Helmholtz equation [41, 42]

$$\Delta H_y(x, z) + k_0^2 n^2(x, I) H_y(x, z) = 0, \quad (2)$$

where $H_y(x, z)$ is the y -component of the magnetic field, Δ is the two-dimensional Laplace operator (in x and z coordinates), k_0 is the wave number in vacuum, and I is the light intensity.

When we choose the y -component of the magnetic field as

$$H_y(x, z) = u(x) \exp(i\beta z),$$

where β is the propagation constant, and $u(x)$ is the field distribution across the film, then the light intensity is given by $I = |u(x)|^2$.

In the case considered, the field distribution $u(x)$ obeys the following equations:

$$u''(x) \pm 2\mu u'(x) + (\beta_p^2 - \beta^2)u(x) = 0, \quad |x| > a, \quad (3)$$

$$u''(x) + (\beta_G^2 - \beta^2)u(x) - (x/x_G)^2 u(x) = 0, \quad |x| < a, \quad (4)$$

where $\beta_p = k_0 n_{p0}$, $\mu = k_0 T / T_p$, $T_p = e / k_0 k_B r_{eff} n_{p0}^4$ [33], $\beta_G = k_0 n_{G0}$, $x_G^2 = a / \beta_G \sqrt{\Delta}$.

The sign "+" in Eq. (3) corresponds to the region $x > a$, and the sign "-" in Eq. (3) corresponds to the region $x < -a$.

The conditions at the film boundaries can be written as:

$$u(\pm a + 0) = u(\pm a - 0), \quad (5)$$

$$u'(a - 0)/n_{G0}^2 = u'(a + 0)/n_{P0}^2, \quad u'(-a - 0)/n_{P0}^2 = u'(-a + 0)/n_{G0}^2, \quad (6)$$

and at infinity: $|u(x)| \rightarrow 0$ at $|x| \rightarrow \infty$.

The solutions to the formulated boundary value problem (3)-(6) describe the waves propagating along the film waveguide. Even ($u(x) = u(-x)$) and odd ($u(x) = -u(-x)$) solutions of this problem can be considered due to the symmetry of the system.

We also calculate the time-averaged total power flow conserving along the waveguide as

$$P = \int_{-\infty}^{+\infty} |u(x)|^2 dx = P_p + P_G, \quad (7)$$

where the component of power flow in the graded-index film is:

$$P_G = 2 \int_0^a |u(x)|^2 dx, \quad (8)$$

and the component of power flow in the photorefractive media is:

$$P_p = 2 \int_a^{\infty} |u(x)|^2 dx. \quad (9)$$

In addition, we analyze the energy redistribution between the waveguide regions across the film direction with relative (percentage) power flows

$$\delta P_{G,p} = P_{G,p} / P, \quad (10)$$

which are also alternative called the radiation confinement (or filling) factors [1].

3. WAVES WITH OSCILLATIONS IN PHOTOREFRACTIVE MEDIUM

We obtain the following even solution to the boundary value problem (3)-(6) in the range $\beta < \min\{\beta_G, \beta_T\}$, where $\beta_T = \sqrt{\beta_p^2 - \mu^2}$ is a "transition point":

$$u_{2m}(x) = u_a \begin{cases} \frac{\cos(p_{2m}(x \mp a \mp x_{2m}))}{\cos(p_{2m}x_{2m})} e^{\mp \mu(x \mp a)}, & |x| > a \\ \frac{H_{2m}(x/x_G)}{H_{2m}(a/x_G)} e^{-(x^2 - a^2)/2x_G^2}, & |x| < a, \end{cases} \quad (11)$$

and the following odd solution to the boundary value problem (3)-(6):

$$u_{2m+1}(x) = u_a \begin{cases} \pm \frac{\cos(p_{2m+1}(x \mp a \mp x_{2m+1}))}{\cos(p_{2m+1}x_{2m+1})} e^{\mp \mu(x \mp a)}, & |x| > a \\ \frac{H_{2m+1}(x/x_G)}{H_{2m+1}(a/x_G)} e^{-(x^2 - a^2)/2x_G^2}, & |x| < a, \end{cases} \quad (12)$$

where u_a is the amplitude at the film interface $x = a$, $m = 0, 1, 2, \dots$,

$$H_j(y) = (-1)^j e^{y^2} \frac{d^j}{dy^j} e^{-y^2},$$

are the Hermite polynomials,

$$p_j = (\beta_r^2 - \beta_G^2 + \beta_G(2j+1)\sqrt{\Delta}/a)^{1/2}, \quad (13)$$

here and below $j = 2m$ for even modes and $j = 2m + 1$ for odd modes,

$$x_j = \frac{1}{p_j} \arctan\left(\frac{\mu + \gamma_j}{p_j}\right), \quad (14)$$

$$\gamma_j = \frac{n_{P0}^2}{n_{G0}^2 x_G} \left\{ \frac{H'_j(\delta)}{H_j(\delta)} - \delta \right\}, \quad (15)$$

where $\delta = a/x_G$.

The upper sign must be chosen in Eqs. (11) and (12) for positive half-space (at $x > a$) and the lower sign must be chosen for negative one (at $x < -a$).

Both even and odd modes exist with the discrete values of propagation constant

$$\beta_j^2 = \beta_G(\beta_G - (2j+1)\sqrt{\Delta}/a), \quad (16)$$

The solutions defined by Eqs. (11) and (12) with parameters (13)-(16) describe even and odd waveguide modes, respectively (we call them modes of the first type), which are characterized by the spatial oscillations (except the ground

mode) inside the film, and attenuation with oscillations in the photorefractive medium with the period

$$\Lambda_j = 2\pi / p_j = 2\pi(\beta_T^2 - \beta_G^2 + \beta_G(2j+1)\sqrt{\Delta/a})^{-1/2},$$

The period Λ_j decreases with an increase in the order of the mode j .

The magnetic field penetrates to a distance of $l = 1/\mu = T_p/Tk_0$ from the film boundary. It is possible to achieve a narrower localization of the light beam near the film along the waveguide by increasing the temperature.

The requirement that the wave number (13) be positive for any orders of modes is satisfied at the temperature $T < T_t$, where

$$T_t = T_p (n_{p0}^2 - n_{G0}^2 + n_{G0}(2j+1)\sqrt{\Delta/ak_0})^{1/2}, \quad (17)$$

and we call it the transition temperature.

The profiles across the film boundaries of even modes defined by Eq. (11) and odd modes defined by Eq. (12) are presented in Figs. 2 and 3, respectively. The spatial profile of main intensity level near the system center is similar to simple soliton solution.

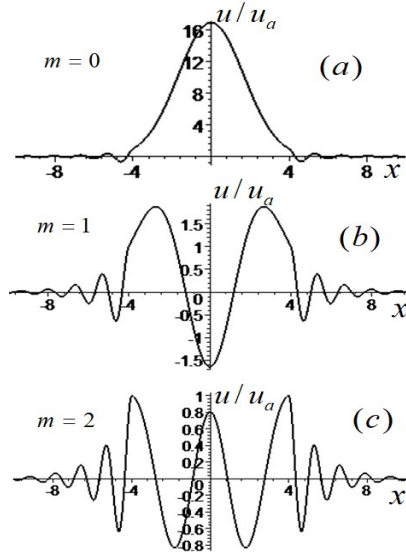


Fig. 2. The profiles of the even modes determined by Eq. (11) with parameters (13)-(16) (in dimensionless conventional units) with $\beta_G = 2$, $\beta_p = 5$, $\Delta = 0.5$, $a = 4$, $\mu = 0.7$, $m = 0$ (a), $m = 1$ (b), $m = 2$ (c).

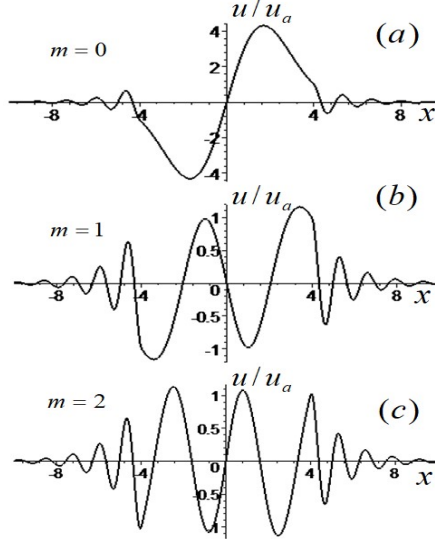


Fig. 3. The profiles of the even modes determined by Eq. (12) with parameters (13)-(16) (in dimensionless conventional units) with the values of the system parameters as in Fig. 2.

The ground mode defined by Eq. (11) with $m = 0$ transforms in the film to the Gaussian function as

$$u_0(|x| < a) = u_a e^{-(x^2 - a^2)/2x_0^2}. \quad (18)$$

The ground mode monotonically attenuates from the film center to its boundaries and it is characterized by one field maximum at the film center. The propagation constant of the ground mode is given by $\beta_0^2 = \beta_G(\beta_G - \sqrt{\Delta}/a)$ (it is obtained from Eq. (16) with $j = 0$). The ground mode is characterized by the largest period $\Lambda_0 = 2\pi(\beta_T^2 - \beta_G^2 + \beta_G)\sqrt{\Delta}/a)^{-1/2}$ at fixed values of the waveguide parameters.

The case of $x_j = 0$ (corresponding to location of the maximum of the light intensity at the film boundaries) is realized when $\gamma_j = -\mu$. This can be achieved at a temperature $T = T_c$, where the critical temperature $T_c = -T_p \gamma_j / k_0$. Note that the values of γ_j can be negative because it is always possible to find the range of δ , for which $H'_j(\delta) < \delta H_j(\delta)$.

4. WAVES WITHOUT OSCILLATIONS IN PHOTOREFRACTIVE MEDIUM

We obtain the even solution to the boundary value problem (3)-(6) in the range $\beta_T < \beta < \min\{\beta_G, \beta_P\}$:

$$u_{2m}(x) = u_a \begin{cases} \frac{\cosh(q_{2m}(x \mp a \mp x_{2m}))}{\cosh(q_{2m}x_{2m})} e^{\mp \mu(x \mp a)}, & |x| > a \\ \frac{H_{2m}(x/x_G)}{H_{2m}(a/x_G)} e^{-(x^2 - a^2)/2x_G^2}, & |x| < a, \end{cases} \quad (19)$$

and the odd solution to the boundary value problem (3)-(6):

$$u_{2m+1}(x) = u_a \begin{cases} \pm \frac{\cosh(q_{2m+1}(x \mp a \mp x_{2m+1}))}{\cosh(q_{2m+1}x_{2m+1})} e^{\mp \mu(x \mp a)}, & |x| > a \\ \frac{H_{2m+1}(x/x_G)}{H_{2m+1}(a/x_G)} e^{-(x^2 - a^2)/2x_G^2}, & |x| < a, \end{cases}, \quad (20)$$

where

$$q_j = (\beta_G^2 - \beta_T^2 - \beta_G(2j+1)\sqrt{\Delta/a})^{1/2}, \quad (21)$$

$$x_j = -\frac{1}{q_j} \tanh^{-1} \left(\frac{\mu + \gamma_j}{q_j} \right). \quad (22)$$

The solutions defined by Eqs. (19) and (21) with parameters (16), (21), and (22) describe even and odd waveguide modes, respectively, which are characterized by the spatial oscillations (except ground mode defined by Eq. (18)) inside the film, and attenuation without oscillations in photorefractive medium. Such modes exist at the temperature $T > T_t$, for which the values of q_j are positives. We call them modes of the second type.

The profiles across the film boundaries of the ground mode defined by Eq. (19) with $m = 0$ ($j = 0$) and the first odd mode defined by Eq. (20) with $m = 0$ ($j = 1$) are presented in Fig. 4 (a) and (b), respectively.

Note that the field in the photorefractive crystal attenuates exponentially for any orders of modes as

$$u(|x| > a) = \pm u_a e^{\mp \mu(x \mp a)}, \quad (23)$$

when the propagation constant (16) coincides with the "transition point" $\beta_j = \beta_T$, which can be realized at the temperature transition $T = T_t$. Such case is often called the "frequency cutoff" because $q_j = p_j = 0$. However, in our case, when the value of

the propagation constant passes through β_T (the temperature passes through T_t , respectively), there is a transition from waves attenuating with oscillations (defined by Eqs. (11) and (12)) to waves attenuating without oscillations (defined by Eqs. (19) and (20)). Therefore, we call β_T the "transition point" and T_t the transition temperature.

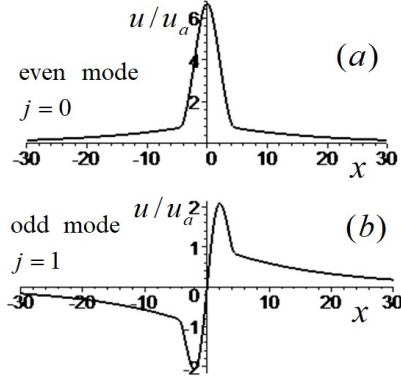


Fig. 4. The profiles of the ground mode determined by Eq. (19) with $m = 0$ ($j = 0$) (a) and the first odd mode defined by Eq. (20) with $m = 0$ ($j = 1$) (b) with parameters (16), (21), and (22) (in dimensionless conventional units) with $\beta_G = \beta_P = 3$, $\Delta = 0.1$, $a = 4$, $\mu = 2$.

5. POWER FLOW ANALYSIS

Combining Eqs. (8) and (11), we calculate the component of power flow of j -mode in the film, which is the same for both types of waves, and it can be written as

$$P_{G_j} = 2u_a^2 x_G e^{\delta x} \frac{F_j(\delta)}{H_j^2(\delta)}, \quad (24)$$

where

$$F_j(\delta) = \int_0^\delta H_j^2(s) e^{-s^2} ds. \quad (25)$$

Combining Eqs. (9) and (11) we calculate the component of power flow in the photorefractive medium of the j -mode of the first type as

$$P_{p_j} = \frac{u_a^2}{2 \cos^2(p_j x_j)} \left\{ \frac{1}{\mu} + \frac{\mu \cos(2p_j x_j) + p_j \sin(2p_j x_j)}{\beta_p^2 - \beta_j^2} \right\}, \quad (26)$$

where x_j is determined by Eq. (14).

Combining Eqs. (9) and (12) we calculate the component of power flow in the photorefractive medium of j -mode of the second type as

$$P_{p_j} = \frac{u_a^2}{2 \cosh^2(q_j x_j)} \left\{ \frac{1}{\mu} + \frac{\mu \cosh(2q_j x_j) - q_j \sinh(2q_j x_j)}{\beta_p^2 - \beta_j^2} \right\}. \quad (27)$$

where x_j is determined by Eq. (22).

Note that the total power (7) of j -mode with components (24), (26) can be written as $P_j = u_a^2 I_j$ where I_j is given by

$$I_j = \left\{ 2x_G e^{\delta^2} \frac{F_j(\delta)}{H_j^2(\delta)} + \frac{1}{2 \cos^2(p_j x_j)} \left(\frac{1}{\mu} + \frac{\mu \cosh(2q_j x_j) - q_j \sinh(2q_j x_j)}{\beta_p^2 - \beta_j^2} \right) \right\}^{-1}.$$

This means that we can choose which of the quantities to consider as the control parameter, namely, the intensity of the light wave at the film boundary u_a^2 or the total flow P_j . In the latter case, one should express the light intensity in terms of the power flow as $u_a^2 = P_j / I_j$.

We find the simple explicit equation of the component of power flow of the ground mode (18) in the film from Eq. (24) as

$$P_{G0} = u_a^2 \sqrt{\pi} x_G e^{\delta^2} \operatorname{erf}(\delta). \quad (28)$$

where $\operatorname{erf}(\delta) = \frac{2}{\sqrt{\pi}} \int_0^\delta e^{-s^2} ds$ is the error function.

The component of power flow of the ground mode of the first type in the photorefractive medium is given by

$$P_{p_0} = \frac{u_a^2}{2 \cos^2(p_0 x_0)} \left\{ \frac{1}{\mu} + \frac{\mu \cos(2p_0 x_0) + p_0 \sin(2p_0 x_0)}{\beta_p^2 - \beta_G^2 + \beta_G \sqrt{\Delta} / a} \right\}. \quad (29)$$

where $p_0 = (\beta_T^2 - \beta_G^2 + \beta_G \sqrt{\Delta} / a)^{1/2}$, $x_0 = \arctan((\mu + \gamma_0) / p_0) / p_0$, and $\gamma_0 = -an_{p_0}^2 / n_{G0}^2 x_G^2$.

The component of the power flow of the ground mode of the second type in the photorefractive medium is given by

$$P_{p0} = \frac{u_a^2}{2 \cosh^2(q_0 x_0)} \left\{ \frac{1}{\mu} + \frac{\mu \cosh(2q_0 x_0) - q_j \sinh(2q_0 x_0)}{\beta_p^2 - \beta_G^2 + \beta_G \sqrt{\Delta} / a} \right\}. \quad (30)$$

where $q_0 = (\beta_G^2 - \beta_G \sqrt{\Delta} / a - \beta_T^2)^{1/2}$, $x_0 = -\tanh^{-1}((\mu + \gamma_0) / q_0) / q_0$.

It is interesting to note that at the critical temperature, when $T = T_c$, Eqs. (26) and (27) coincide with each other, and transform into

$$P_{pj} = \frac{u_a^2}{2} \left(\frac{1}{\mu_c} + \frac{\mu_c}{\beta_p^2 - \beta_j^2} \right). \quad (31)$$

where $\mu_c = k_0 T_c / T_p = -\gamma_j$.

The dependencies of the total power flow (7) with the components defined by Eqs. (24) and (26) on the film thickness are presented in Fig. 5. The corresponding relative power flows δP_{Gj} and δP_{pj} are presented in Fig. 6. The total power flow reaches a minimum value at a certain value of the film thickness. On one hand, this means that the corresponding waveguide mode can only be excited when the energy of the exciting beam is greater than the critical value of the total power. On the other hand, this means that the wave energy can be minimized by choosing a film thickness close to the critical value.

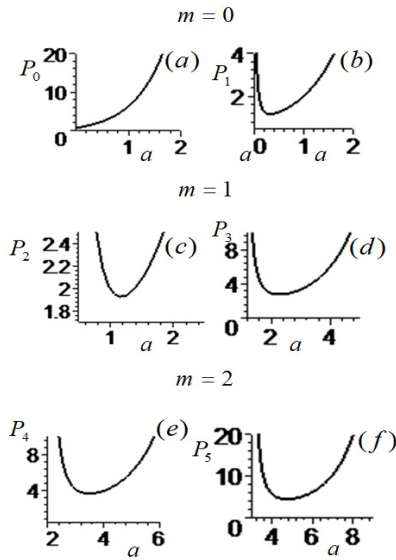


Fig. 5. The total power (7) with the components defined by Eqs. (24) and (26) versus film thickness with different orders of even and odd modes with $j=0$ (a), $j=1$ (b), $j=2$ (c), $j=3$ (d), $j=4$ (e), $j=5$ (f) and the values of parameters as in Fig. 2.

The analysis of relative flows shows that a large fraction of the energy is concentrated in the photorefractive plates at small film thicknesses. In this case we observe $\delta P_{G_j}(a) < \delta P_{p_j}(a)$ (Fig 6.). The fraction $\delta P_{p_j}(a)$ decreases, and the fraction of energy concentrated in the film $\delta P_{G_j}(a)$ increases with the growth of its thickness. The fraction of energy in the film begins to exceed the fraction of energy in the photorefractive medium. In this case we observe $\delta P_{G_j}(a) > \delta P_{p_j}(a)$. Note that the dependences $\delta P_{G_j}(a)$ and $\delta P_{p_j}(a)$ are not monotonic and maxima and minima are observed starting from the second-order modes (from $m=1$). Their number grows with the growth of the mode order. Further redistribution of energy between the film and the medium of the plates does not occur. We observe that $\delta P_{G_j}(a) \rightarrow 1$ and $\delta P_{p_j}(a) \rightarrow 0$ with the further increase in the value of a .

Thus, we can obtain a wave with an energy flow density concentrated in the outer photorefractive coatings of the waveguide by choosing a film thickness less than a critical one. If the film thickness is greater than the critical one, then a wave will be obtained with the energy flow density of the waveguide core concentrated in the graded-index film.

The dependence on the film thickness is similar for other types of waves and their analysis does not require special attention.

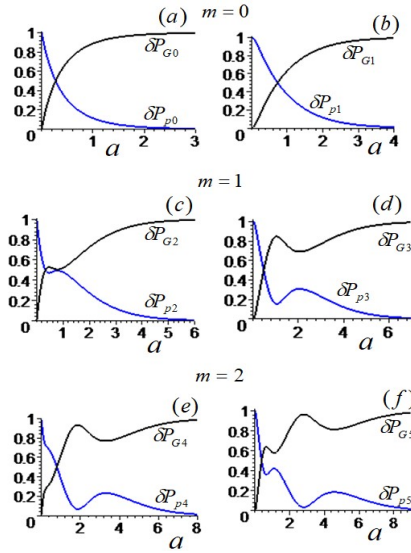


Fig. 6. The relative power flows δP_{G_j} and δP_{p_j} of even and odd modes with the components defined by Eqs. (24) and (26) versus film thickness with $j = 0$ (a), $j = 1$ (b), $j = 2$ (c), $j = 3$ (d), $j = 4$ (e), $j = 5$ (f) and the values of parameters as in Fig. 2.

6. DISCUSSION

Let us note three of our previous articles that are closest in geometry and structure to the waveguide symmetrical three-layer structure [33, 43-45]. In these papers, symmetrical three-layer planar structures were considered, the outer layers of which consist of photorefractive crystals with the same optical characteristics, and the inner layer has different optical properties from outer layers. In particular, a dielectric interlayer with a constant refractive index is considered in [43]. The interlayer characterized by the Kerr nonlinearity is considered in [44]. The closest internal layer in terms of characteristics [45], in which the refractive index is symmetrically distributed according to a linear equation

$$n_G^2(x) = n_{G0}^2 \{1 - \Delta|x|/a\}, \quad (32)$$

is considered in [33].

Due to symmetry, in such systems there are surface waves with a transverse field distribution, characterized by a certain symmetry relative to the interfaces of the layers, in particular, in-phase and anti-phase modes, described by even and odd solutions, respectively. In the present paper, attention is paid to the analysis of the conditions of existence and energy characteristics of surface waves and waveguide modes of TM polarization in contrast to Ref. [33] where the energy flux was not calculated.

In the mentioned papers, only the case of negligibly low dark intensity compared to the intensity of the surface wave was considered. Then the effective attenuation coefficient becomes constant at $I_d \ll I$ [40]. Such a limiting case (as an oscillator with constant friction) was considered in [41, 42] when studying the excitation of surface waves propagating along the surface of a photorefractive crystal in contact with air, where two types of attenuation of surface waves were described.

Surface waves are described by solutions of equation (2) with different index profile $n_G(x)$ in Eq. (1), coupled with the boundary conditions (6) at the layer interfaces of the waveguide structure. The solutions for the outer layers in all papers [33, 43-45] are the same in form. The differences lie in solutions for the inner layers. Consequently, surface waves are described by fundamentally different expressions in different papers. In particular, in Ref. [43] the solution for the inner layer was described by cosine/sine in one range of the varying propagation constant and by hyperbolic cosine/sine in another one. In Ref. [44] the solution for the inner layer was described by elliptic functions in different ranges of the varying propagation constant.

The solution for the inner layer was described by Airy function in [33]. Let us consider in more detail the comparison of the case of a linear graded-index inner

layer with a parabolic one. In the case of $n > n_{G0}$ the symmetric solution to Eq. (2) with (32) is given by

$$H_j(x) = H_{jm} \text{Ai}(|x|/x_G + \delta_j) \quad (33)$$

where $j = 1, 2, \dots$, Ai is the Airy function, δ_j are the zeros of the derivative of the Airy function, $\delta = -(n_{G0}^2 - (\beta/k_0)^2)(ak_0/n_{G0}\Delta)^{2/3}$, $x_G = (a/k_0^2 n_{G0}^2 \Delta)^{1/3}$, and the amplitude H_{jm} was found from the boundary conditions [45]. The wave defined by Eq. (33) can propagate with the discrete spectrum of the propagation constant $\beta_j = (n_{G0}^2 - n_{Sj}^2)^{1/2} / k_0$, where $n_{Sj}^2 = |\delta_j| (n_{G0}^2 \Delta / ak_0)^{2/3}$.

The anti-symmetric solution to Eq. (2) with (32) is given by

$$H_j(x) = \pm H_{jm} \text{Ai}(|x|/x_G + \xi_j) \quad (34)$$

where ξ_j are the zeros of the Airy function. The wave defined by Eq. (34) can propagate with the discrete spectrum of the propagation constant $\beta_j = (n_{G0}^2 - n_{Aj}^2)^{1/2} / k_0$, where $n_{Aj}^2 = |\xi_j| (n_{G0}^2 \Delta / ak_0)^{2/3}$.

The Eqs. (33) and (34) describe the waveguide modes. The generation of high order modes is controlled by the thickness of the inner layer. However, these expressions differ significantly from equations (11), (12), (19), and (20) obtained in this work. As a consequence of this, the wave profiles obtained in this paper differ from the wave profiles described by (33) and (34). The same can be stated for the localization width of the light flux along the waveguide.

In other planar symmetrical waveguide structures we described earlier [15, 36, 45], in which the outer plates were either linear dielectrics or characterized by Kerr nonlinearity, the field in the transverse direction decreased exponentially with distance from the layer interfaces. Therefore, the waves found in this paper are new, to the best of our knowledge. We also refer here to some recent works on the unique properties of surface and guided waves in other physical settings [46-49].

7. CONCLUSIONS

We described theoretically the waveguide properties of the film with a parabolic spatial profile of the refractive index inserted in a medium with diffusion type of photorefractive nonlinearity. We found two new types of guided waves with a spatial profile localized along the film boundaries. We obtained exact solutions to the wave equation corresponding to even and odd modes. The wave of the first type attenuates with oscillations in the photorefractive coating media and the second one attenuates without oscillations. The wave types also differ from each other by the range of values of the propagation constant. We found that all

modes exist at certain discrete values of the propagation constant, which depend on the optical parameters of the system and the film thickness.

We calculated analytically the total power flow of all types of modes and analyzed the effect of the film thickness. We found that the corresponding waveguide mode can only be excited when the energy of the exciting beam is greater than the critical value of the wave total power flow. A large fraction of the energy is concentrated in the photorefractive plates at small film thicknesses. The redistribution of energy between the film and the medium of the plates occurs with an increase in the film thickness. A large fraction of the energy is concentrated in the film at its thicknesses more than the critical one.

We showed that a wave with an energy flow density concentrated in the outer photorefractive coatings of the waveguide can be obtained by choosing a film thickness less than the critical one and a wave with the energy flow density concentrated in the graded-index film of the waveguide core is obtained by choosing its thickness greater than the critical one.

The possibility of the existence of waves with oscillating attenuation of the field amplitude fundamentally distinguishes heterostructures based on optical media with a photorefractive effect from layered structures consisting of graded-index optical media. The way indicated in this paper for controlling oscillations and adjusting the depth of field energy localization along the layers can be useful in the development of various optical devices based on the use of photorefractive and graded-index induced properties of crystals in multilayer structures.

REFERENCES

1. M. J. Adams, *An Introduction to Optical Waveguides*, Wiley, Chichester, 481 (1981).
2. C. Lavers, *Journal of Physics: Conference Series*, **178**, 012010 (2009).
3. L. Lan, L. Li, X. Yang, P. Naumov, H. Zhang, *Adv. Funct. Mater.* **32**, 2211760 (2022).
4. V. Prajzler, P. Nekvindová, P. Hys, O. Lyutakov, V. Jerabek, *Radioengineering* **23**, 776-782 (2014).
5. M. Bednarik, M. Cervenka, *J. Opt. Soc. Am. B* **37**, 3631 – 3643 (2020).
6. J. M. Kubica, *Opt. Quant. Electron.* **55**, 137 (2023).
7. D. Mihalache, M. Bertolotti, C. Sibilia, *Prog. Opt.* **27**, 229 – 313 (1989).
8. V. Bhairavabhatla, S. Talabattula, 2008 IEEE/LEOS Winter Topical Meeting Series, 18 – 19 (2008).
9. D. J. Robbins, *Optics Communications* **47**, 309 – 312 (1983).
10. J.-L. Coutaz, M. Kull, *J. Opt. Soc. Am. B* **8**, 95 – 98 (1991).
11. V. Kursseva, S. Tikhov, D. Valovik, *Journal of Nonlinear Optical Physics & Materials* **28**, 1950009 (2019).
12. N. N. Beletsky, E. A. Hasan, *Phys. of the Sol. St.* **36**, 647 – 652 (1994).
13. S. E. Savotchenko, *Rom. Rep. Phys.* **72**, 412 (2020).
14. S. E. Savotchenko, *Rom. Rep. Phys.* **74**, 407 (2022).
15. S. E. Savotchenko, *Rom. J. Phys.* **65**, 202 (2020).
16. Z. Luo, F. Liu, Y. Xu, H. Liu, T. Zhang, J. Xu, J. Tian, *Opt. Express* **21**, 15075 – 15080 (2013).

17. D. Kh. Nurligareev, B. A. Usievich, V. A. Sychugov, L. I. Ivleva, *Quantum Electronics* **43**, 14 – 20 (2013).
18. A. B. Shvartsburg, A. Maradudin, *Waves in Gradient Metamaterials*, World Scientific, Singapore, 339 (2013).
19. A. Sharma, J.-P. Meunier, *Optical and Quantum Electronics* **34**, 377 – 392 (2002).
20. N. A. Kudryashov, *Optik* **224**, 165391 (2020).
21. T. Touam, F. Yergeau, *Appl. Opt.* **32**, 309 – 312 (1993).
22. S.-Y. Huang, S. Wang, *Journal of Applied Physics* **55**(4), 647 – 651 (1984).
23. M. H. Weik, *Computer Science and Communications Dictionary*. Springer, Boston, 1104 (2000).
24. B. B. Svendsen, M. Söderström, H. Carlens, M. Dalarsson, *Appl. Sci.* **12**, 7097 (2022).
25. V. K. Fedyanin, D. Mihalache, *Z. Phys. B* **47**, 167 – 173 (1982).
26. D. Mihalache, G. I. Stegeman, C. T. Seaton, E. M. Wright, R. Zanoni, A. D. Boardman, T. Twardowski, *Opt. Lett.* **12**, 187 – 189 (1987).
27. E. Conwell, *Appl. Phys. Lett.* **25**, 40 (1974).
28. A. H. M. Almagani, S. A. Taya, A. J. Hussein, I. Colak, *J. Opt. Soc. Am. B* **39**, 1606 – 1613 (2022).
29. A. J. Hussein, S. A. Taya, D. Vigneswaran, R. Udiyakumar, A. Upadhyay, T. Anwar, I. S. Amiri, *Results in Physics* **20**, 103734 (2021).
30. S. A. Taya, A. J. Hussein, O. M. Ramahi, I. Colak, Y. B. Chaouche, *J. Opt. Soc. Am. B* **38**(11), 3237 – 3243 (2021).
31. S. E. Savotchenko, *Optik* **271**(12), 170092 (2022).
32. S. E. Savotchenko, *Mathematical Modelling of Natural Phenomena* **20**(1), 1 (2025).
33. S. E. Savotchenko, *Applied Physics B: Lasers and Optics* **129**(1), 7 (2023).
34. S. E. Savotchenko, *Physica B* **648**(1), 414434 (2023).
35. D. G. Sannikov, D. I. Sementsov, A. M. Shutyi, *Russ. Phys. J.* **44**, 442 – 444 (2001).
36. S. E. Savotchenko, *Physica E* **147**(3), 115622 (2023).
37. A. M. Shutyi, D. I. Sementsov, A. V. Kazakevich, D. G. Sannikov, *Tech. Phys.* **44**(11), 1329 – 1333 (1999).
38. D. G. Sannikov, D. I. Sementsov, A. M. Shutyi, A. V. Kazakevich, *Tech. Phys. Lett.* **25**, 977 – 979 (1999).
39. A. M. Shutyi, D. I. Sementsov, D. G. Sannikov, *Russ. Phys. J.* **43**, 601 – 607 (2000).
40. S. A. Chetkin, I. M. Akhmedzhanov, *Quantum Electronics* **41**, 980 – 985 (2011).
41. B. A. Usievich, D. Kh. Nurligareev, V. A. Sychugov, L. I. Ivleva, P. A. Lykov, N. V. Bogodaev, *Quantum Electronics* **40**, 437 – 440 (2010).
42. B. A. Usievich, D. Kh. Nurligareev, V. A. Sychugov, L. I. Ivleva, *Quantum Electronics* **41**(10), 924 – 928 (2011).
43. S. E. Savotchenko, *Quantum Electronics* **49**(9), 850 – 856 (2019).
44. S. E. Savotchenko, *Solid State Communications* **296**(7), 32 – 36 (2019).
45. S. E. Savotchenko, *Russ. Technol. J.* **12**(5), 77 – 89 (2024).
46. B. A. Malomed, D. Mihalache, *Rom. J. Phys.* **64**, 106 (2019).
47. D. Mihalache, *Rom. Rep. Phys.* **73**, 403 (2021).
48. D. Mihalache, *Rom. Rep. Phys.* **76**, 402 (2024).
49. S. E. Savotchenko, *Rom. J. Phys.* **69**, 201 (2024).